Novel Hybrid Photocatalyst for Visible-light-sensitive CO_2 Reduction: Direct Assembly Synthesis of a Metal-complex on Spherical Mesoporous Semiconductor Particles

Tomiko M. Suzuki, Tadashi Nakamura, Shu Saeki, Yoriko Matsuoka, Hiromitsu Tanaka, Shunsuke Sato, Kazuhisa Yano, Tsutomu Kajino and Takeshi Morikawa

Report received on Aug. 4, 2013

■■**ABSTRACT**‖ We report on the synthesis of highly effective hybrid photocatalysts for CO_2 reduction, where a metal-complex was used to modify the mesopores of *p*-type, N-doped Ta_2O_5 (N-Ta_2O_5) spheres. A direct assembly method was developed for the synthesis of the hybrid photocatalysts anchored with organic groups, which provides for a quicker and simpler preparation than conventional methods. The photocatalyst consists of a Ru-complex and fine non-porous N-Ta_2O_5 particles anchored by phosphonate groups and exhibits excellent activity for the photoconversion of CO_2 to HCOOH in acetonitrile/triethanolamine solution under visible light irradiation with respect to the reaction rate and stability. The turnover number for the formation of HCOOH was 4.9 times higher than that for previously reported photocatalysts anchored by carboxylate.

Furthermore, to improve the photocatalytic activity of N-Ta_2O_5, novel hierarchical structured, submicron-sized mesoporous N-Ta_2O_5 spheres (N-CMTS) assembled from N-Ta_2O_5 nanocrystals were successfully synthesized by a sol-gel process, followed by heat-treatment with the aid of carbon reinforcement and nitridation. In the case of N-CMTS used as a semiconductor for the hybrid photocatalyst system, the amount of HCOOH generated by CO_2 photoreduction was still more than 1.5 times higher than that of fine nonporous N-Ta_2O_5 particles used as a semiconductor, due to the higher surface area and controlled morphology of N-CMTS. This work could facilitate the design and synthesis of highly efficient photocatalysts for solar energy conversion and solar fuel production.

■■**KEYWORDS**‖ Photocatalyst, Visible Light, Tantalum Pentoxide, Nitrogen Doping, Metal-complex, Mesoporous, Spherical Particle, CO_2 Reduction, Formic Acid

1. Introduction

The development of photocatalysts to convert CO_2 into useful organic chemicals under irradiation with sunlight is increasingly important in respect of the fossil fuel shortage and global warming problem. Among the renewable energy resources, solar energy is by far the largest exploitable resource, which provides more energy per hour to the Earth than the total energy consumed by the global population in one year.

We have successfully constructed a system for solar CO_2 reduction to organic chemicals such as formate using H_2O as both an electron donor and proton source.[1–4] The point of breakthrough for this artificial photosynthetic process was to achieve highly selective reduction of CO_2 in an aqueous medium utilizing a hybrid photocatalyst composed of a semiconductor photosensitizer and a metal-complex electrocatalyst.[1,5] The photocatalytic process involves the transfer of

electrons in the photoexcited semiconductor from the conduction band to the metal-complex catalyst, which leads to the selective reduction of CO_2 over the metal-complex.[5] Accordingly, the solar reduction of CO_2 to formate in water was accomplished by the so-called Z-scheme (two-step photoexcitation) reaction, in which a photocathode for CO_2 reduction and a photoanode for water oxidation are connected electrically.[1]

It is also important to develop a heterogeneous system of particles for the practical future of this artificial photosynthetic system to achieve highly efficient solar CO_2 reduction. During the initial stage of hybrid catalyst development, fine particles of a *p*-type semiconductor, N-doped Ta_2O_5 (N-Ta_2O_5), were developed with a band gap of 2.4 eV.[6] N-Ta_2O_5 is a very useful material to perform fundamental research on semiconductor/metal-complex hybrid photocatalysts because visible-light-induced electrons can be transferred to many complexes, due to its highly

negative conduction band minimum (E_{CBM}) located at -1.3 V vs. NHE (normal hydrogen electrode).[6,7] Consequently, we have successfully demonstrated proof of concept for the selective visible-light-induced reduction of CO_2 in acetonitrile (MeCN) /triethanolamine (TEOA) solution utilizing a combination of ruthenium-complex electrocatalysts[8,9] and N-Ta_2O_5 particles.[7]

A simple mixture of the of N-Ta_2O_5/Ru-complex hybrid system exhibited lower CO_2 photoreduction activity. In contrast, when the Ru-complex was anchored by carboxylate onto N-Ta_2O_5, the CO_2 reduction rate was significantly improved due to the acceleration of electron transfer by both direct linkage and an increase of the driving force, ΔG between E_{CBM} and the CO_2 reduction potential of the complex (**Fig. 1**).[7,10] Therefore, it is considered that an appropriate choice of anchoring groups between the semiconductor and metal-complex can enhance the activity for CO_2 reduction due to enhancement of the electron transfer rate between them. The increase in surface area of the semiconductor could also effectively enhance the reaction rate.

Herein, we report on the successful improvement of CO_2 photoreduction activity of the semiconductor/metal-complex particle system: (1) development of a direct synthesis method of the metal-complex onto the semiconductor particle surface, which is applicable to efficient screening of optimal anchoring groups, (2) synthesis of morphologically controlled mesoporous N-Ta_2O_5
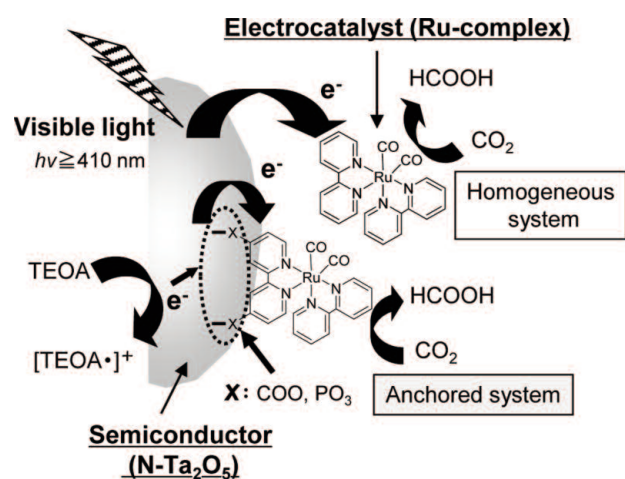
spheres (N-CMTS) with high surface area and their application as CO_2 reduction photocatalysts.

2. Direct Assembly Synthesis of Hybrid Photocatalysts: Direct Formation of Metal-complex Catalysts on Semiconductor Surfaces

Further investigation of optimal anchoring groups between the metal-complex and semiconductor is essential to improve the rate for photocatalytic CO_2 reduction because it enhances both the electronic structure at the interface and the driving force, ΔG, which determines the rate for electron transfer from a semiconductor to the metal-complex. Hybrid materials of semiconductor and metal-complex with an anchoring group are typically prepared by adsorption of the metal-complex onto the semiconductor surface (adsorption method), such as with various dye/TiO_2 hybrids for dye-sensitized solar cells (DSSCs)[11–13] and CO_2 reduction photocatalysts previously developed by the authors.[7] To determine the optimal anchoring groups, metal-complexes containing anchoring groups with different chemical structures and properties must be individually synthesized. However, the limited solubility of polar groups attached to the semiconductor can prove to be disadvantageous with respect to handling and purification of the materials, which often makes it difficult to synthesize metal-complexes with anchoring groups.[10]

An alternative approach for binding the metal-complex to the semiconductor particle is the direct assembly of the metal-complex on a ligand-functionalized semiconductor by electrostatic interaction (direct assembly method). This method should result in the intended complex forming reaction with less side reactions, but this has been reported in only a few papers.[14] In the present work, we synthesized Ru-complex/N-Ta_2O_5 composites that were anchored by organic groups using the direct assembly method, and examined the effects of the anchoring group on the rate for the photoreduction of CO_2 in acetonitrile solution.

2. 1 Experimental

2. 1. 1 Materials

4,4'-Dicarboxy-2,2'-bipyridine ([dcbpy]) and TEOA were obtained from Sigma-Aldrich (USA) and used as

Fig. 1 Mechanism for the reduction of CO_2 by photocatalysis under visible light with a Ru-complex/N-Ta_2O_5 hybrid catalyst.

received. Dimethylformamide (DMF), dimethylsulfoxide (DMSO), and dehydrated MeCN were purchased from Wako Pure Chemical Co. (Japan). 4,4'-diphosphonate-2,2'-bipyridine ([dpbpy]), $[Ru(bpy)(CO)_2(CF_3SO_3)_2]$, and $[Ru(bpy)_2(CO)_2]^{2+}$ $(PF_6^-)_2$ ([Ru-bpy]) were synthesized according to procedures in the literature.[15,16] $N-Ta_2O_5$ powder was prepared by annealing Ta_2O_5 powder under NH_3 flow at 848 K for 6 h.[6,7]

2. 1. 2 Direct Synthesis of Ru-complex onto N- Ta_2O_5

$N-Ta_2O_5$ with adsorbed [dcbpy] ([dcbpy]/$N-Ta_2O_5$) was prepared by shaking a mixture of $N-Ta_2O_5$ (500 mg) and 0.65 mM [dcbpy] solution in DMF (10 mL) overnight. $N-Ta_2O_5$ with adsorbed [dpbpy] ([dpbpy]/$N-Ta_2O_5$) was prepared by shaking a mixture of $N-Ta_2O_5$ (500 mg) and 1.5 mM [dpbpy] solution in DMSO (10 mL) overnight. These solutions were centrifuged, washed several times, and dried in vacuo at 313 K. The UV/vis adsorption spectra of the supernatants were measured (Shimadzu UV-3600) and the amount of ligand adsorbed on $N-Ta_2O_5$ was calculated. [dcbpy]/$N-Ta_2O_5$ or [dpbpy]/$N-Ta_2O_5$ (400 mg) and $[Ru(bpy)(CO)_2(CF_3SO_3)_2]$ (2 equiv. vs. adsorbed ligand) were mixed in ethanol under N_2 and refluxed for 5 h. The solution was filtered, washed, and dried in vacuo to obtain [Ru-dcbpy]/$N-Ta_2O_5$ or [Ru-dpbpy]/$N-Ta_2O_5$.

2. 1. 3 Evaluation of Catalyst Structure and Photocatalytic Reaction

Attenuated total reflectance-Fourier transform infrared (ATR-FTIR) spectra of the catalyst samples were measured (Bruker Optics VERTEX 80). The Ru content in the samples was determined by inductively coupled plasma spectroscopy (ICP) analysis (Rigaku CIROUS 120 EOP).

Photocatalytic activity was measured at ambient pressure in 8 mL test tubes containing 4 mL of a dehydrated MeCN/TEOA (5/1 = v/v) and 10 mg of photocatalyst. After purging with CO_2 for 15 min, the solutions were irradiated using a 500 W Xe lamp with filters to produce light in the range of $410 \leq \lambda \leq 750$ nm at room temperature, as reported previously.[7] Product concentrations were determined using gas chromatography (Shimadzu GC-14A) and ion-exchange chromatography (Dionex ICS-2000).

2. 2 Results and Discussion

2. 2. 1 Structural Analysis of Hybrid Photocatalysts

Scheme 1 shows the Ru-complex/semiconductor ($N-Ta_2O_5$) hybrid photocatalyst synthesized by complexing of Ru-complex onto bipyridine-functionalized $N-Ta_2O_5$. The Ru-complex was attached to $N-Ta_2O_5$ via carboxylate or phosphonate functional groups. The chemical structures of the composites were characterized using ATR-FTIR spectroscopy. **Figure 2** shows spectra for $N-Ta_2O_5$, [Ru-dpbpy]/$N-Ta_2O_5$, their difference spectrum, and that for [Ru-bpy]. Bands originating from the carbonyl group (2081, 2018, 2000 cm^{-1}) were clearly observed in the spectrum of [Ru-dpbpy]/$N-Ta_2O_5$. Similar results were obtained for [Ru-bpy] without an anchor group. In addition, the band from phosphonate (1157 cm^{-1}) was observed in the difference spectrum. These results indicate that the Ru-complex was synthesized on $N-Ta_2O_5$ by the direct assembly method. The successful synthesis of
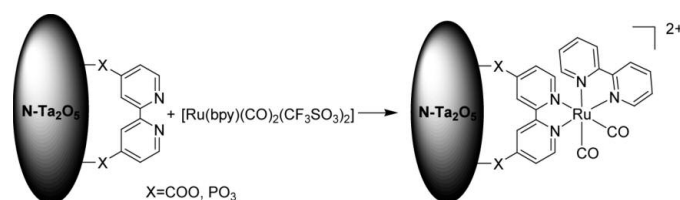
Scheme 1   Ru-complex assembled on bipyridine (bpy)-functionalized $N-Ta_2O_5$ (direct assembly method).
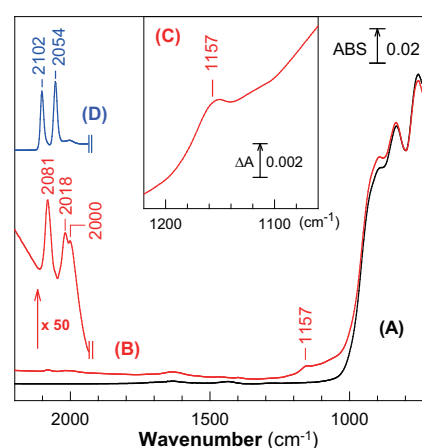
Fig. 2   ATR-FTIR spectra for (A) $N-Ta_2O_5$, (B) [Ru-dpbpy]/$N-Ta_2O_5$, (C) difference spectrum (B-A), and (D) [Ru-bpy].

[Ru-dcbpy]/N-Ta$_2$O$_5$ was also confirmed by similar ATR-FTIR measurements. Direct connection of the Ru-complex and N-Ta$_2$O$_5$ via organic groups was also verified using time-of-flight secondary ion mass spectrometry (TOF-SIMS; data not shown).[10]

2. 2. 2 Photocatalytic CO$_2$ Reduction Over Hybrid Catalysts Under Visible-light Irradiation

Photocatalytic CO$_2$ reduction of the hybrid materials was performed in MeCN/TEOA solution under visible-light irradiation. The main photocatalytic product was confirmed to be HCOOH, as previously reported.[7] **Figure 3** shows the turnover number (TN) for the formation of HCOOH from CO$_2$ per metal-complex (TN$_{HCOOH}$) of [Ru-dcbpy]/N-Ta$_2$O$_5$ and [Ru-dpbpy]/ N-Ta$_2$O$_5$ as a function of irradiation time. TN$_{HCOOH}$ (at 60 h) over [Ru-dcbpy]/N-Ta$_2$O$_5$ prepared by the direct assembly method was confirmed to be the same level as that over [Ru-dcbpy]/N-Ta$_2$O$_5$ prepared by the conventional adsorption method which [Ru-dcbpy] complex was directly adsorbed onto N-Ta$_2$O$_5$.[10] However, the direct assembly method provides a quicker and more simple preparation than that of the adsorption method. In the case of [Ru-dcbpy]/N-Ta$_2$O$_5$, the formation of formic acid plateaued after 16 h. In contrast, the photocatalytic activity of [Ru-dpbpy]/N-Ta$_2$O$_5$ anchored by

phosphonate groups was more efficient than that of the photocatalysts anchored by carboxylate groups from the early stage (inset) and was maintained even after 60 h of photoreaction. After 60 h of photoreaction, TN$_{HCOOH}$ over [Ru-dpbpy]/N-Ta$_2$O$_5$ was approximately 4.9 times higher than over the [Ru-dcbpy]/N-Ta$_2$O$_5$ photocatalyst anchored by carboxylate groups.

The higher activity and stability of the photocatalyst anchored by phosphonate groups than that anchored by carboxylate groups could be possibly explained by the following reasons: (1) A phosphonate anchoring group can provide a strong chemical linkage to a metal oxide surface over a wide pH range.[12] (2) The lower CO$_2$ reduction potential of [Ru-dpbpy] compared to that of [Ru-dcbpy], which was verified by cyclic voltammetry using hybrid electrodes with Ru-complexes immobilized on TiO$_2$-coated fluorine-doped tin dioxide (FTO) glass (data not shown), increases ΔG, which results in efficient electron transfer from N-Ta$_2$O$_5$ to [Ru-dpbpy].[10]

In summary, the hybrid catalyst anchored with phosphonate groups exhibited the highest CO$_2$ reduction rate and stability of the Ru-complex/N-Ta$_2$O$_5$ systems. Therefore, in section 3, the direct assembly synthesis is applied to a semiconductor with mesopores to realize an active CO$_2$ reduction photocatalyst.

3. Synthesis of Mesoporous N-doped Ta$_2$O$_5$ Spheres for a Highly Efficient Photocatalyst

Fine *p*-type N-Ta$_2$O$_5$ particles that absorb visible light at wavelengths shorter than 500 nm[6] were developed and selective visible-light-induced reduction of CO$_2$ to HCOOH was accomplished by utilizing a combination of this semiconductor and a Ru-complex. The size of the fine N-Ta$_2$O$_5$ particles was estimated to be 20–40 nm and the specific surface area was 19 m^2 g^{-1}.

Control of morphology and particle size is required to enhance the photocatalytic activity of N-Ta$_2$O$_5$, as demonstrated for mesoporous silica or TiO$_2$ catalysts.[17–20] Higher surface area can enhance the interaction of N-Ta$_2$O$_5$ with the reactants, while the submicron-sized spherical morphology composed of nanocrystals is expected to enhance optical absorption due to light scattering, such as with ZnO or TiO$_2$ spheres.[21–23]

Therefore, submicron-sized mesoporous N-Ta$_2$O$_5$ aggregates consisting of N-Ta$_2$O$_5$ nanocrystals are
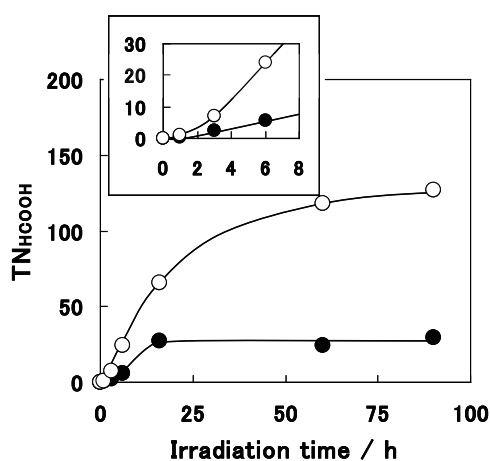

Fig.3 Turnover number (TN) for the formation of HCOOH from CO$_2$ as a function of irradiation time over the [Ru-dcbpy]/N-Ta$_2$O$_5$ (●) and [Ru-dpbpy]/N-Ta$_2$O$_5$ (○) catalysts. TN$_{HCOOH}$ = mmol HCOOH/mmol Ru-complex in the hybrid catalyst. The inset shows TN$_{HCOOH}$ during the initial stage.

expected to be an ideal candidate photocatalyst. Although the syntheses of irregular-shaped crystallized mesoporous Ta_2O_5 and ammonia-treated Ta_3N_5 have been reported,[24–26] there have been no reports on the synthesis of spherical crystallized mesoporous Ta compounds assembled from nanocrystals. **Scheme 2** shows the strategy employed to construct a novel hierarchical structure that provides both nanocrystals and mesopores: (1) synthesis of amorphous mesoporous Ta_2O_5 spheres, (2) crystallization of as-prepared mesoporous Ta_2O_5 by heat-treatment with the aid of carbon reinforcement, and (3) nitridation of crystallized mesoporous Ta_2O_5. Herein, we propose a new route to synthesize visible-light-sensitive mesoporous $N-Ta_2O_5$ spheres (N-CMTS) that exhibit enhanced photocatalytic activity.

3. 1 Experimental

3.1.1 Materials

All starting materials were used as received. Tantalum pentaethoxide ($Ta(OEt)_5$) was purchased from Sigma-Aldrich (USA). Octadecylamine was purchased from Tokyo Kasei Co. (Japan). Ethylene glycol, methanol, ethanol, hydrochloric acid, and furfuryl alcohol were purchased from Wako Pure Chemical Co. (Japan).

3. 1. 2 Synthesis of Amorphous Mesoporous Ta_2O_5 Spheres (MTS)

The MTS were prepared by a modified ligand-assisted templating method,[27,28] in which a mixture of $Ta(OEt)_5$ (12.3 mmol) and octadecylamine (6.15 mmol)

Scheme 2 Procedure for the synthesis of N-CMTS.

was hydrolyzed in 1000 g of water/organic solvent. After 5 h of continuous stirring, the resulting white powder (Ta_2O_5/surfactant composite) was filtered and added to 25 mL of water in a Teflon-lined autoclave. The hydrothermal synthesis procedure was the same as that reported for the original ligand-assisted templating method.[28] To remove the surfactant, 1 g of the resulting powder was heated in 100 mL of ethanol solution containing 1 mL of concentrated hydrochloric acid at 333 K for 3 h. The resultant powder was filtered, washed, and dried at 318 K.

### 3. 1. 3 Preparation of Crystallized MTS (CMTS) and N-doped CMTS (N-CMTS)

Furfuryl alcohol was used as a carbon source.[29,30] Furfuryl alcohol was impregnated into the mesopores of MTS and subsequently polymerized in air at 423 K for 24 h. The sample was then heat-treated at 1073 K for 1 h under a nitrogen atmosphere to obtain a crystallized MTS (CMTS)/carbon composite. Calcination of the composite at 823 K for 5 h in air yielded crystallized MTS (CMTS). N-CMTS was prepared by annealing CMTS under NH_3 flow at 848 K for 6 h.

3. 1. 4 Synthesis of Ru-complex [Ru-dpbpy]/N-CMTS Hybrid Photocatalyst

Hybrid photocatalysts consisting of a ruthenium complex $[Ru(dpbpy)(bpy)(CO)_2]^{2+}$ and N-CMTS were synthesized using the direct assembly method (section 2. 1. 2).

3. 1. 5 Characterization of Catalyst Structure and Photocatalytic Reaction for Hydrogen Evolution and CO_2 Reduction

Scanning electron microscopy (SEM) and field emission-SEM (FE-SEM) images were obtained with Akashi Seisakusho SIGMA-V and Hitachi FE-SEM S-5500 microscopes, respectively. Nitrogen adsorption isotherms were measured using a particle analyzer (BEL Japan Belsorp-mini II) at 77 K. Powder X-ray diffraction (XRD) measurements were conducted using a Rigaku Rint-TTR diffractometer with Cu Kα radiation. The N 1 *s* and O 1 *s* core levels were measured using X-ray photoelectron spectroscopy (XPS; Ulvac-Phi Quantera SXM) with monochromated Al Kα radiation to determine the N states and
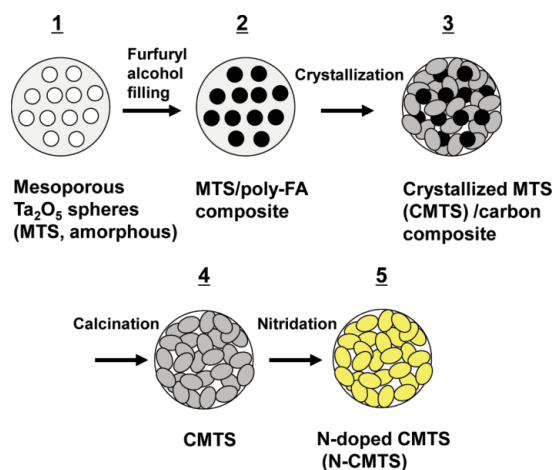
N-doping concentrations. The Ru content in the samples was determined by ICP analysis (Rigaku CIROS 120 EOP).

Photocatalytic activity was measured as described in section 2.1.3. For the measurement of the hydrogen evolution, the solution was purged with Ar gas.

3. 2 Results and Discussion

3. 2. 1 Synthesis of N-CMTS

Amorphous mesoporous Ta_2O_5 is conventionally synthesized by a ligand-assisted templating method using a Ta source and surfactant.[27,28] However, irregular-shaped aggregates of the precipitate were obtained because of the fast hydrolysis and condensation rates of the Ta source under solvent-free or low-solvent conditions. Therefore, the synthesis of amorphous Ta_2O_5 particles was conducted by modification of this method, where a mixture of Ta(OEt)$_5$-octadecylamine was hydrolyzed in a dilute solution of water/organic solvent to control the hydrolysis and condensation reaction rates. The morphology of the amorphous mesoporous Ta_2O_5 was significantly affected by the solvent composition during the hydrolysis of Ta(OEt)$_5$, and separate submicron-sized spherical particles (MTS) were obtained for the first time using water/methanol/ethylene glycol solution (**Fig. 4**(a)).[31] The N_2 adsorption isotherm for MTS was identified as type IV, which is typical for mesoporous materials. The BET specific area and pore diameter analyzed by the
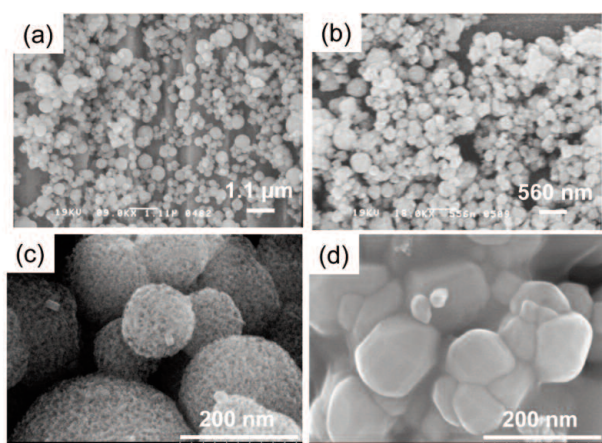
Fig. 4 SEM images of (a) MTS synthesized using water/methanol/ethylene glycol (30:50:20) and (b) CMTS heat-treated at 1073 K. FE-SEM images of CMTS heat-treated at 1073 K (c) with and (d) without carbon-reinforcement.

Barrett-Joyner-Halenda (BJH) method were 460 m^2 g^{-1} and 3.4 nm, respectively.[31] The unique spherical Ta_2O_5 particles were considered to result from the addition of high-viscosity ethylene glycol, which affects the hydrolysis, condensation rate of Ta(OEt)$_5$, and the dispersibility of the formed particles.[32]

CMTS have been prepared by reinforcing MTS with carbon and calcining the CMTS/carbon composite. The resultant CMTS was heat-treated at 1073 K and retained the spherical morphology of MTS, as shown in Fig. 4(b). The FE-SEM image shown in Fig. 4(c) indicates that the spherical particles consist of Ta_2O_5 nanoparticles of ca. 10 nm. The particle structures were also confirmed by TEM observation (data not shown).[31] When heat-treatment was performed without carbon-infilling, the morphology of the particles was entirely changed and large primary particles (40−200 nm) were obtained (Fig. 4(d)). This result strongly suggests that carbon plays an important role in retaining the spherical morphology of the MTS and formation of the nanocrystals during the phase change. XRD patterns (data not shown) of the resultant CMTS have broad peaks typical for orthorhombic Ta_2O_5 and the average crystallite size was estimated to be 12.8 nm using Scherrer's equation, which agrees well with that determined from the FE-SEM and TEM images.[31] The CMTS had a relatively high specific surface area (105 m^2 g^{-1}) and mesopores with an average diameter of 5.6 nm (**Table 1**) after crystallization of Ta_2O_5. During the calcination of the CMTS/carbon composite, carbon was removed by combustion, and interparticle nanospaces were generated between Ta_2O_5 nanocrystals. The pore diameter of CMTS was controllable in the range of 5.6−17 nm by changing the crystallization temperature.[31]

The yellowish N-CMTS almost retained mesoporosity and the same morphology of CMTS and the nitrogen concentration was determined to be 5.0 at% by XPS (Table 1). XRD peaks for N-CMTS were unchanged and no peaks of TaON or Ta_3N_5 were detected as previously reported,[6] which demonstrates that N-doping of orthorhombic CMTS was successfully achieved. In addition, the XPS spectral peaks around 400 and 396.6 eV indicated that N-CMTS is a p-type semiconductor, as we recently confirmed.[6] Hence, the energy positions of the conduction band minimum (E_{CBM}) and the valence band maximum (E_{VBM}) of N-CMTS are likely to be located at −1.3 V (vs. NHE) and +1.1 V, respectively.

3. 2. 2 Photocatalytic Hydrogen Evolution and CO$_2$ Reduction Using N-CMTS

To investigate the effect of the relatively high surface area and morphology of N-Ta$_2$O$_5$ on the photocatalytic activity, photocatalytic H$_2$ evolution reactions were performed over N-CMTS in MeCN/TEOA pre-purged with Ar gas under visible-light ($\geq$ 410 nm) irradiation for 24 h and the results are summarized in Table 1. For comparison, fine non-porous N-Ta$_2$O$_5$ particles (N-Ta$_2$O$_5$, as described in section 2) was also evaluated. N-CMTS exhibited photocatalytic activity for H$_2$ evolution that was 2.1 times higher than that for N-Ta$_2$O$_5$ due to the higher surface area and controlled morphology. In addition, the photocatalytic activity of N-CMTS was maintained even after 72 h of photoreaction, which is due to the stability of N-Ta$_2$O$_5$ photocatalyst.[31]

Hybrid photocatalysts for CO$_2$ reduction that consisted of Ru-complexes and N-CMTS anchored by phosphonate ([Ru-dpbpy]/N-CMTS) were successfully synthesized by the direct assembly method, as confirmed by ATR-FTIR spectroscopy (see section 2). The maximum Ru content of [Ru-dpbpy]/N-CMTS (0.12 wt% Ru) determined by ICP analysis was higher than that of [Ru-dpbpy]/N-Ta$_2$O$_5$ containing 0.07 wt% Ru, which suggests that the higher surface area

of N-CMTS enabled the incorporation of more [Ru-dpbpy] than N-Ta$_2$O$_5$. The specific surface area and pore size of [Ru-dpbpy]/N-CMTS (0.12 wt% Ru) were measured after the incorporation of [Ru-dpbpy], and were decreased from 86 m^2 g^{-1} and 6.8 nm to 70 m^2 g^{-1} and 6.4 nm, respectively, which indicates that the Ru-complex was successfully incorporated into the mesopores of N-CMTS.[31]

Table 2 summarizes the results for photocatalytic CO$_2$ reduction over the hybrid photocatalysts in MeCN/TEOA solution under visible-light ($\geq$ 410 nm) irradiation. For all hybrid samples, the main photocatalytic reaction product from CO$_2$ was HCOOH. The amounts of HCOOH generated over [Ru-dpbpy]/N-CMTS and [Ru-dpbpy]/N-Ta$_2$O$_5$-fine with the same quantities of Ru (0.05 wt%) were almost similar, irrespective of the mesoporosity (4.7 and 4.4 μmol), which strongly indicates that photocatalytic CO$_2$ reduction occurs on the Ru-complex incorporated in the mesopores of N-CMTS. The amount of HCOOH generated over [Ru-dpbpy]/N-Ta$_2$O$_5$ with the highest Ru content (0.07 wt%) was very close to that of [Ru-dpbpy]/N-Ta$_2$O$_5$ with lower Ru content (0.05 wt%). The limit of [Ru-dpbpy] content is provided by the trade-off between the surface area required for simultaneous CO$_2$ reduction and TEOA oxidation to occur on N-Ta$_2$O$_5$ particles. The

Table 1 Physical properties and photocatalytic activities of mesoporous Ta$_2$O$_5$ and N-doped Ta$_2$O$_5$ samples for H$_2$ evolution under visible-light irradiation (410 $\leq \lambda \leq$ 750 nm).

Sample	N content (at. %)[a]	Pore volume (ml/g)	Specific surface area (m^2/g)	Pore diameter (nm)	H$_2$ evolved (μmol)
CMTS	–	0.16	105	5.6	0.02
N-CMTS	5.0	0.14	86	6.8	1.31
N-Ta$_2$O$_5$	5.3	–	19	–	0.63

[a] Estimated by XPS analysis.

Table 2 Photocatalytic activities of N-CMTS and N-Ta$_2$O$_5$ photocatalysts with Ru-complex for CO$_2$ reduction under visible-light irradiation (410 $\leq \lambda \leq$ 750 nm).

Sample	Ru content (wt%)[a]	HCOOH evolved (μmol)
N-CMTS	0.05	4.7
	0.12	7.1
N-Ta$_2$O$_5$	0.05	4.4
	0.07	4.6

[a] Estimated by ICP analysis.

coverage of [Ru-dpbpy] in [Ru-dpbpy]/N-Ta$_2$O$_5$ containing 0.05 wt% Ru was estimated to be ca. 16%. However, the amount of HCOOH generated over [Ru-dpbpy]/N-CMTS containing 0.12 wt% Ru was 1.5 times higher than that for [Ru-dpbpy]/N-CMTS containing 0.05 wt% Ru, which also indicates that the Ru-complex incorporated into the mesopores of N-CMTS takes part in the CO$_2$ photoreduction. This is because the optimum loading of [Ru-dpbpy], which was determined by the balance between CO$_2$ reduction and TEOA oxidation, was increased with the higher surface area of N-CMTS.

It has not yet been clarified if the submicron-sized spherical morphology of N-CMTS improves the optical absorption by a light-scattering effect. However, it is confirmed that a porous *p*-type semiconductor with high specific surface area composed of nanocrystals could be beneficial for future solar conversion technology, because sufficient space is available for the incorporation of functional materials such as metal-complex catalysts, co-catalysts, and other semiconductor nanoparticles.

4. Conclusions

Novel hybrid photocatalysts of Ru-complexes and *p*-type photoactive N-Ta$_2$O$_5$ anchored with their respective organic groups were successfully synthesized by a direct assembly method. The hybrid photocatalysts exhibited activity and efficient photoconversion of CO$_2$ to HCOOH under visible-light irradiation in MeCN/TEOA. The direct assembly method provides quick and simple catalyst preparation with competitive photocatalytic activity to that of the conventional method. The photoactivity and stability of the hybrid photocatalysts were dependent on the chemical structure of the anchor group, and that anchored by phosphonate groups exhibited excellent photocatalytic activity with respect to the reaction rate and stability. This work could also be extended to the synthesis of various types of hybrid materials consisting of metal-complexes and inorganic materials applicable to future solar conversion technology.

To improve the photocatalytic activity of N-Ta$_2$O$_5$, submicron-sized N-CMTS assembled from N-Ta$_2$O$_5$ nanocrystals was synthesized. Photocatalysts composed of N-CMTS and a Ru-complex anchored by phosphonate groups exhibited excellent photocatalytic activity for CO$_2$ reduction in MeCN/TEOA under visible-light irradiation due to the stronger anchoring effect of phosphonate groups, high surface area, and controlled morphology of the mesoporous N-Ta$_2$O$_5$ spheres. The proposed methodology is simple, versatile, and applicable to the synthesis of various types of crystallized mesoporous spherical semiconductors for solar conversion technology.

The valence band maximum (VBM) of N-Ta$_2$O$_5$ (+1.1 V vs. NHE) is insufficient for water oxidation by electron extraction (+1.23 V); therefore, TEOA was used as an electron source to compensate for the photogenerated hole in N-Ta$_2$O$_5$. TEOA is used as both an electron donor and a proton source to produce formic acid from CO$_2$. However, the information elucidated in the present paper can also be applied to semiconductor/metal-complex systems for the conversion of CO$_2$ into useful organic chemicals under irradiation with sunlight using H$_2$O as both an electron donor and a proton source, and this investigation is currently in progress.

References

(1) Sato, S., Arai, T., Morikawa, T., Uemuram K., Suzuki, T. M., Tanaka, H. and Kajino, T., *J. Am. Chem. Soc.*, Vol. 133, No. 39 (2011), pp. 15420-15243.
(2) Arai, T., Tajima, S., Sato, S., Uemura, K., Morikawa, T. and Kajino, T., *Chem. Commun.*, Vol. 47, No. 47 (2011), pp. 12664-12666.
(3) Arai, T., Sato, S., Kajino, T. and Morikawa, T., *Energy Environ. Sci.*, Vol. 6, No. 4 (2013), pp. 1274-1282.
(4) Kajino, T., Morikawa, T., Sato, S., Arai, T., Suzuki T. M., Uemura, K., Yamanaka, K., Saeki, S. and Tanaka, H., *R&D Review of Toyota CRDL,* Vol. 43, No. 2 (2012), pp. 43-52.
(5) Arai, T., Sato, S., Uemura, K., Morikawa, T., Kajino, T. and Motohiro, T., *Chem. Commun.*, Vol. 46, No. 37

(2011), pp. 6944-6946.

(6) Morikawa, T., Saeki, S., Suzuki, T., Kajino, T. and Motohiro, T., *Appl. Phys. Lett.*, Vol. 96, No. 14 (2010), pp. 142111-142113.

(7) Sato, S., Morikawa, T., Saeki, S., Kajino, T. and Motohiro, T., *Angew. Chem. Int. Ed.*, Vol. 49, No. 30 (2010), pp. 5101-5105.

(8) Ishida, H., Terada, T., Tanaka, K. and Tanaka, T., *Organometallics*, Vol. 96, No. 1(1987), pp. 181-186.

(9) Tanaka, K., *Bull. Chem. Soc. Jpn.,* Vol. 71, No. 1 (1998), pp. 17-29.

(10) Suzuki, T. M., Tanaka, H., Morikawa, T., Iwaki, M., Sato, S., Saeki, S., Inoue, M., Kajino, T. and Morohiro, T., *Chem. Commun.*, Vol. 47, No. 30 (2011), pp. 8673-8675.

(11) O'Regan, B. and Grätzel, M., *Nature*, Vol. 353, No. 6346 (1991), pp. 737-740.

(12) Park, H., Bae, E., Lee, J. J., Park, J. and Choi, W., *J. Phys. Chem. B.*, Vol. 110, No. 17 (2006), pp. 8740-8749.

(13) Hagfeldt, A., Boschloo, G., Sun, L., Kloo, L. and Pettersson, H., *Chem. Rev.,* Vol. 110, No. 11 (2010), pp. 6595-6663.

(14) Brumbach, M. T., Boal, A. K. and Wheeler, D. R., *Langmuir*, Vol. 25, No. 18 (2009), pp. 10685-10690.

(15) Penicaud, V., Odobel, F. and Bujoli, B., *Tetrahedron Lett.*, Vol. 39, No. 22 (1998), pp. 3689-3692.

(16) Anderson, P. A., Deacon, G. B., Haarmann, K. H., Keene, F. R., Meyer, T. J., Reitsma, D. A., Skelton, B. W., Strouse, G. F., Thomas, N. C., Treadway, J. A. and Whit, A. H., *Inorg. Chem.*, Vol. 34, No. 24 (1995), pp. 6145-6157.

(17) Suzuki, T. M., Yamamoto, M., Fukumoto, K., Akimoto, Y. and Yano, K., *J. Catal.*, Vol. 251, No. 2 (2007), pp. 249-257.

(18) Suzuki, T. M., Nakamura, T., Sudo, E., Akimoto, Y. and Yano, K., *Microporous Mesoporous Mater.*, Vol. 111, No. 1-3 (2008), pp. 350-358.

(19) Sakatani, Y., Grosso, D., Nicole, L., Boissière, C., Soler-Illia, G. J. A. A. and Sanchez, C., *J. Mater. Chem.,* Vol. 16, No. 1 (2006), pp. 77-82.

(20) Chen, X. and Mao, S. S., *Chem. Rev.*, Vol. 107, No. 7 (2007), pp. 2891-2959.

(21) Zhang, Q, Chou, T. P., Russo, B., Jenekhe S. A. and Cao, G., *Adv. Funct. Mater.*, Vol. 18, No. 11 (2008), pp. 1654-1660.

(22) Chen, D., Huang, F., Cheng, Y.-B. and Caruso, R. A., *Adv. Mater.,* Vol. 21, No. 21 (2009), pp. 2206-2210.

(23) Kim, Y. J., Lee, M. H., Kim, H. J., Lim, G., Choi, Y. S., Park, N.-G., Kim, K. and Lee, W. I., *Adv. Mater.*, Vol. 21, No. 36 (2009), pp. 3668-3673.

(24) Kondo, J. N. and Domen, K., *Chem. Mater.*, Vol. 20, No. 3 (2008), pp. 835-847.

(25) Noda, Y., Lee, B., Domen, K. and Kondo, J. N., *Chem. Mater.*, Vol. 20, No. 16 (2008), pp. 5361-5367.

(26) Hisatomi, T., Otani, M., Nakajima, K., Teramura, K., Kako, Y., Lu, D., Takata, T., Kondo, J. N. and Domen, K., *Chem. Mater.*, Vol. 22, No. 13 (2010),

pp. 3854-3861.

(27) Antonelli, D. M. and Ying, J. Y., *Chem. Mater.*, Vol. 8, No. 4 (1996), pp. 874-881.

(28) Kondo, J. N., Takahara, Y., Lu, D. and Domen, K., *Chem. Mater.*, Vol. 13, No. 4 (2001), pp. 1200-1206.

(29) Nakamura, T., Yamada, Y. and Yano, K., *Chem. Lett.*, Vol. 35, No. 12 (2006), pp. 1436-1437.

(30) Nakamura, T., Yamada, Y. and Yano, K., *Microporous Mesoporous Mater.*, Vol. 117, No. 1-2 (2009), pp.478-485.

(31) Suzuki, T. M., Nakamura, T., Saeki, S., Matsuoka, Y., Tanaka, H., Yano, K., Kajino, T. and Morikawa, T., *J. Mater. Chem.,* Vol. 22, No. 47 (2012), pp. 24584-24590.

(32) Yamada, Y. and Yano, K., *Microporous Mesoporous Mater.*, Vol. 93, No. 1-3 (2006), pp. 190-198.

Figs. 1-3 and Scheme 1
Reprinted from Chem. Commun., Vol. 47, No. 30 (2011), pp. 8673-8675, Suzuki, T. M., Tanaka, H., Morikawa, T., Iwaki, M., Sato, S., Saeki, S., Inoue, M., Kajino, T. and Morohiro, T., Direct Assembly Synthesis of Metal Complex-semiconductor Hybrid Photocatalysts Anchored by Phosphonate for Highly Efficient CO_2 Reduction, © 2011 The Royal Society of Chemistry.

Scheme 2
Reprinted from J. Mater. Chem., Vol. 22, No. 47 (2012), pp. 24584-24590, Suzuki, T. M., Nakamura, T., Saeki, S., Matsuoka, Y., Tanaka, H., Yano, K., Kajino, T. and Morikawa, T., Visible Light-sensitive Mesoporous N-doped Ta_2O_5 Spheres: Synthesis and Photocatalytic Activity for Hydrogen Evolution and CO_2 Reduction, © 2012 The Royal Society of Chemistry.

Tomiko M. Suzuki
  Research Fields:
    - Photocatalysis
    - Functional Materials Chemistry
  Academic Degree: Dr.Eng.
  Academic Societies:
    - American Chemical Society
    - The Chemical Society of Japan
    - Catalysis Society of Japan
    - The Society of Polymer Science, Japan
  Awards:
    - Tokai Chemical Industry Association Award, 2000
    - J.B.B. Best Paper Award, The Society for Biotechnology, Japan, 2007
    - 14th International Congress on Catalysis Pre-symposium, Best Poster Presentation Award, 2008
    - Best Poster Presentation Award, 109th Meeting of Catalysis Society of Japan, 2012
    - Best Poster Presentation Award, 111th Meeting of Catalysis Society of Japan, 2013

Tadashi Nakamura
Research Fields:
- Inorganic Materials Chemistry
- Solid State Electrochemistry
Academic Degree: Dr.Eng.
Academic Societies:
- The Chemical Society of Japan
- The Ceramic Society of Japan
- The Electrochemical Society of Japan
Award:
- Award of Outstanding Papers of The Ceramic Society of Japan, 2005

Shu Saeki
Research Fields:
- Photocatalysis
- Functional Inorganic Materials
Academic Degree: Dr.Eng.
Academic Society:
- The Society of Powder Technology, Japan

Yoriko Matsuoka
Research Field:
- Materials Analysis by Scanning Electron Microscope

Hiromitsu Tanaka
Research Fields:
- Organic Functional Materials
- Application of Carbon Materials
Academic Degree: Dr.Eng.
Academic Societies:
- American Chemical Society
- The Chemical Society of Japan

Shunsuke Sato
Research Fields:
- Photocatalyst
- Photochemistry of Coordination Compounds
Academic Degree: Ph.D.
Academic Societies:
- The Chemical Society of Japan
- The Photofunctional Complexes Research Association
Award:
- The Chemical Society of Japan Presentation Award, 2013

Kazuhisa Yano
Research Fields:
- Porous Materials
- Colloidal Crystal
Academic Degree: Dr.Eng.
Academic Society:
- American Chemical Society

Tsutomu Kajino
Research Fields:
- Solar Fuel Production
- Catalytic Chemistry
Academic Degree: Dr.Agr.
Academic Societies:
- The Chemical Society of Japan
- The Society for Biothechnology, Japan
Awards:
- R&D 100 Award, 2002
- Technology Development Award of Japan Fine Ceramics Association, 2005

Takeshi Morikawa
Research Fields:
- Photocatalysis
- Semiconductor Physics
Academic Degree: Dr.Eng.
Academic Societies:
- IEEE
- The Chemical Society of Japan
Awards:
- R&D 100 Award, 1993
- Technology Development Award of Japan Fine Ceramics Association, 2003
- Award of Outstanding Papers of The Ceramic Society of Japan, 2005
- The Ceramic Society of Japan Technology Award, 2006
- American Ceramic Society Corporate Environmental Achievement Award, 2006
- The Chemical Society of Japan Award for Technical Development, 2007